Cosmic Ray Anisotropy Workshop 2013 (CRA2013) IOP Publishing
Journal of Physics: Conference Series **531** (2014) 012003 doi:10.1088/1742-6596/531/1/012003

Galactic magnetic deflections of UHECRs including realistic random fields

Azadeh Keivani[1], Glennys Farrar[2], Michael Sutherland[1,3,4] and James Matthews[1]

[1]Department of Physics & Astronomy, Louisiana State University, Baton Rouge, LA
[2]Center for Cosmology and Particle Physics, New York University, New York, NY
[3]Department of Physics, The Ohio State University, Columbus, OH
[4]Center for Cosmology and AstroParticle Physics, The Ohio State University, Columbus, OH

E-mail: akeivani@phys.lsu.edu

Abstract. We present the results of a study that simulates trajectories of ultra-high energy cosmic rays from Centaurus A to Earth. The arrival directions are characterized to assess whether Cen A can be identified as a source of cosmic rays based on observing departures from isotropy. We analyze separately particles originating from the central engine as well as from the north and south radio lobes of the Cen A complex. Simulations are performed for particle rigidities from $E/Z = 2$ EV to 100 EV, thus covering the possibility of primary particles as heavy as Fe nuclei with energies exceeding 50 EeV. The Galactic magnetic field is modeled using the recent work of Jansson and Farrar (JF12) which fitted its parameters to match extragalactic Faraday rotation measures and WMAP7 synchrotron emission maps. We also discuss the effects of an additional turbulent magnetic field on the cosmic ray deflections.

1. Introduction

One of the biggest mysteries in particle astrophysics is the origin of ultra-high energy cosmic rays (UHECRs). There are few source types that appear capable of accelerating the particles to energies as high as has been observed ($> 10^{20}$ eV). Moreover, UHECRs with energies above 5×10^{19} eV (50 EeV) lose energy through interactions with cosmic microwave background photons so that any that are observed must have originated within about 200 Mpc [1, 2]. Centaurus A (Cen A) is the closest active galactic nucleus (AGN) to Earth and is one of these source candidates. The Pierre Auger Observatory has reported a modest excess of cosmic ray arrival directions from within about 20° of the celestial location of Cen A in their UHECR data [3]. This greatly increases the interest to study the propagation of UHECRs through the Galactic magnetic fields (GMF) from Cen A.

UHECRs are mostly or entirely charged particles [4] so they will be deflected in the magnetic fields that they traverse on their way to Earth. In this study, we simulate trajectories of cosmic rays from Cen A to Earth to examine the deflections that occur due to the GMF. We construct the GMF according to the new model of Jansson and Farrar [5, 6] (JF12). The parameters of the JF12 model were tuned to give an excellent global fit to observed rotation measures and polarized synchrotron data. An overview of the model is given in Section 2.

This study is an extension to the work of Farrar *et al.* [7], where they simulated UHECRs from center of Cen A with different rigidities (energy divided by the particle's charge: $R = E/Z$)

of 160, 80, 40 and 20 EV. Here we simulate additional and lower rigidities down to 2 EV from the center of Cen A as well as considering the northern and southern radio lobes. Another important addition is studying the effects of adding a new, detailed Kolmogorov random field component to the coherent JF12 GMF model.

Cen A was proposed to be the possible source of most cosmic rays by Farrar and Piran [8] assuming constraints on the values of turbulent extragalactic magnetic fields (See also [9]). Since the Pierre Auger Observatory released its first set of UHECR events, there have been several studies on the correlation of UHECRs with Cen A. For example, Gorbunov *et al.* discuss the possibility that Cen A could be the source of a significant part of the observed events [10]. Wibig and Wolfendale assume that all observed UHECRs were from three sources including Cen A [11]. Hardcastle *et al.* argue the possibility that the giant radio lobes of Cen A could accelerate UHECRs [12]. Other related works are described in [13–19].

The propagation method is briefly explained in Section 3 and the results of the simulation are discussed in Section 4.

2. JF12 GMF model

JF12 is a new GMF model that has been fitted to the WMAP7 Galactic synchrotron emission map [20] and more than forty thousand extragalactic rotation measures to constrain its parameters. This model includes a large scale regular component, a so-called "striated" random component that is generally arranged to follow the larger geometric features of the regular component [5], and a turbulent random field component [6]. In this study, we first consider the large scale regular component of the JF12 model. The component contains a disk field component, a toroidal halo component and an out-of-plane component as suggested by observations of external galaxies. Then, for a subset of rigidities, we add to this a turbulent random field realization characterized by a Kolmogorov power spectrum.

The r.m.s. magnitude of the random component of the JF12 model varies in space. At any point it is proportional to the magnitude of the regular component of the spiral arm structure at that location. In their study, they did not construct actual realizations of the random field due to their analysis method for constraining the field magnitudes. UHECR propagation requires such a realization so we have developed a method for propagation by creating first a small (spatial) box that contains a grid of field magnitudes which follow a Kolmogorov spectrum. Copies of this box are placed throughout the GMF volume. Each box then has its internal field magnitudes scaled according to the JF12 random component r.m.s. strength at that point. The total magnetic field is the vector sum of the regular and random field vectors. Independent random field realizations can be constructed by generating new boxes with different random number seeds.

3. Tracking

We use the latest release (v3.0.4) of *CRT* [21] which is a program to inject and propagate UHECRs from various galactic and extragalactic sources through the GMF models. *CRT* uses adaptive Runge-Kutta integration methods to determine the trajectory of a charged particle through a magnetic field according to the relativistic Lorentz force.

The method we use to track the cosmic rays through the GMF is "backtracking" particles from the Earth and recording their location and velocities when they exit the Galactic field region. Backtracking is accomplished by following the anti-particle, which simply means changing the sign of the particle's charge and reversing the incoming velocity vector. The propagation of a particle stops when it hits the pre-defined boundary of the Galaxy since the extragalactic magnetic field is assumed to have negligible magnitude in this study.

We backtrack a fixed number of cosmic rays from isotropically distributed initial locations using HEALPix [22]. HEALPix is an acronym for Hierarchical Equal Area isoLatitude

Pixelization of a sphere. In this study, we pick HEALPix resolution index 11 which defines more than 5×10^7 pixels each covering 8×10^{-4} deg^2. We backtrack one particle from the center of each pixel with a fixed rigidity R. An event with rigidity R could be a proton with energy R or an iron nucleus with energy $26R$. Several different rigidities are considered starting with $\log(R_{\rm EV})$=2 (or $R = 100$ EV) and ending at $\log(R_{\rm EV})$=0.3 (or $R \simeq 2.0$ EV) in steps of 0.05 in $\log(R)$.

UHECRs are simulated isotropically over the whole sky as described above. We identify particles of different rigidities that backtrack to regions of celestial solid angle within a radius of 3° around a chosen source location; in the first case this is the center of Cen A. The Larmor radius of a relativistic charged particle in a magnetic field B is simply given by R/B, so the use of rigidity R allows a single simulation to represent a variety of primary particle compositions with appropriately scaled total primary energies. We repeat the process for source locations centered on the tips of the northern and southern radio lobe.

4. Event Excess from Cen A

The backtracking process begins by sending (anti)particles outward in all directions. We keep for further study only those trajectories that intercept the Cen A region. This is defined by a solid angle surface with angular radius of 3° around the center of Cen A. Such a size includes a good portion of the radio galaxy which may be likely sites of acceleration and emission of cosmic rays. Since Cen A is about 3.8 Mpc away from the Earth, the 3° circle encompasses a physical distance of about 200 kpc in radius from the center, roughly midway between the central engine and the limits of the outer radio lobes which lie about 500 kpc from the center.

In the backtracking method, any particle that emerges from the volume where we have defined the Galactic magnetic field with a velocity vector pointing to the defined region around Cen A is retained for analysis. Its launch direction is then an arrival direction for a particle with opposite charge but the same rigidity accelerated at Cen A. Figure 1 shows the arrival direction distribution of the simulated events with $R = 56.23$ EV. The centroid and standard deviations of longitude and latitude of the events are shown as the black point and lines respectively. The particles are propagated through only the regular component of JF12 in this section.

The process is repeated for 35 different values of rigidity. Figure 2 shows the centroids and standard deviations of the arrival direction distributions from the center of Cen A for all simulated rigidities. Each color represents a different rigidity as indicated in the legend. These points illustrate how the arrival directions of UHECRs from the center of Cen A deviate from the source direction as a function of the rigidity of the particle. Particles with large R values deviate much less than those with smaller values. Note that for $R < 17.78$ EV, the arrival directions branch into two distinct regions on the plot; the centroid and standard deviations of such split distributions are computed and plotted separately.

An alternative hypothesis is that the northern and/or southern tips of the Cen A radio lobes are the location(s) of the source accelerator. We separately study the directions of the simulated events coming from within 3° near the tips of the northern and southern radio lobes. We find that the general stream of the events are the same, but the appearance of separated regions split away from the main thread begins at lower rigidities ($R = 12.59$ EV) for the northern tip source and at higher rigidities ($R = 22.39$ EV) for the southern tip source. The main thread is shifted towards greater latitude values for the source at the northern tip and is shifted towards smaller latitude values for the source at the southern tip, comparing to the source at the center of Cen A. These shifts are only a few degrees for the lower rigidities. The shape and orientation of the threads remain the same as for the center of Cen A source case, in the sense that lower rigidities trail towards lower longitude and latitude values. The separate regions observed for lower rigidities shift primarily in longitude by about ten degrees but maintain the same curved rigidity ordering and structure.

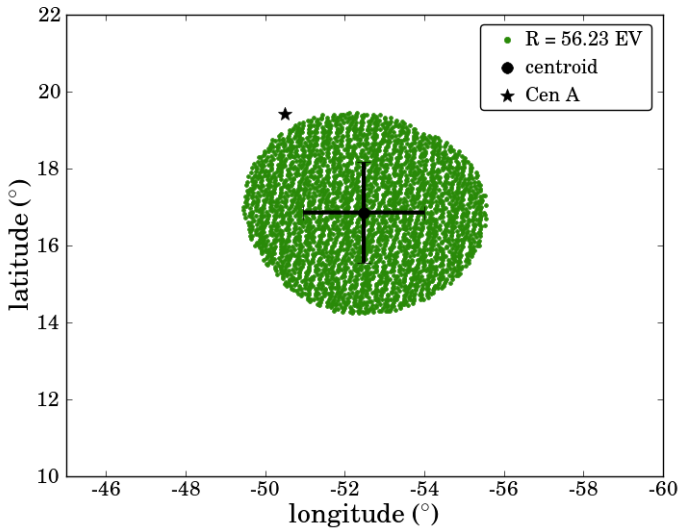

Figure 1. Directions of the simulated events with $R = 56.23$ EV originating from within 3° around the center of Cen A. The centroid and the standard deviations of these events are shown.

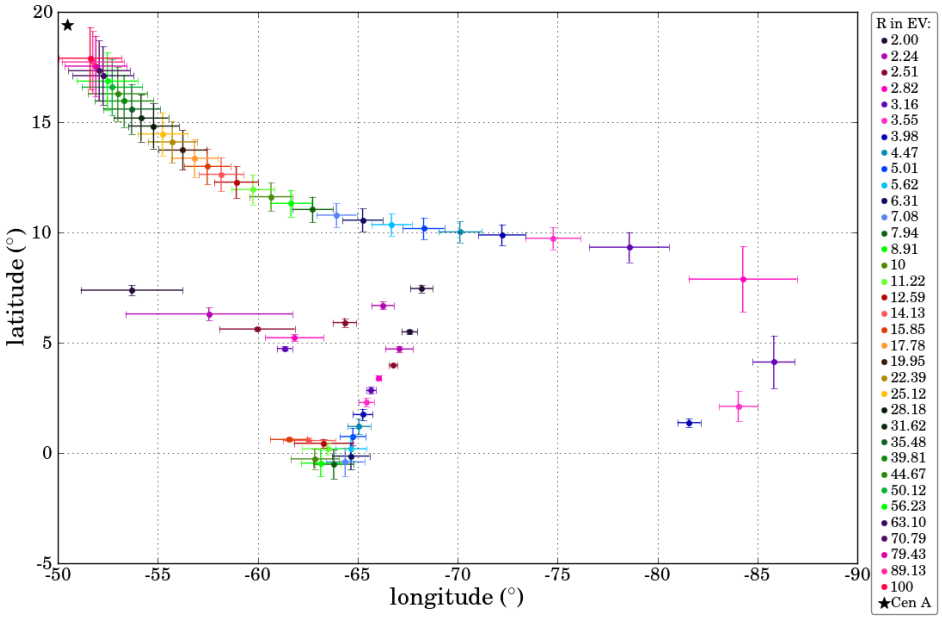

Figure 2. Centroids of the directions of the simulated events within 3° of the vicinity of the center of Cen A in Galactic coordinates. The error bars indicate the standard deviation of events with same rigidity.

The Pierre Auger Observatory has reported an excess of events (with respect to isotropic expectations) above 55 EeV within about 20° around Cen A [3]. This motivates us to examine the same quantity with our simulated arrival direction distributions.

We calculate the fraction of simulated events arriving within an angle ψ from a specified

source direction and compare with what would be expected if arrival directions were isotropic and uncorrelated. This is done separately for the three simulation sets corresponding to the assumed Cen A source locations (north, center, or south).

To compare the Auger results, we will be interested in ultra-high energy events with energies above 55 EeV. If we assume all the particles are protons, then we will only consider simulated events with $R \geq 56.23$ EV and include all the simulated rigidities up to 100 EV in this case. On the other hand, if the events are assumed to be all iron nuclei, then the minimum simulated rigidity that we will use is $R = 2.24$, corresponding to $E \approx 58$ EeV. As very few events have ever been observed above 100 EeV, when considering iron nuclei we impose a somewhat arbitrary upper limit on the rigidities used at 7.08 EV, corresponding to a primary energy in that case of 26×7.08 EeV $= 184$ EeV.

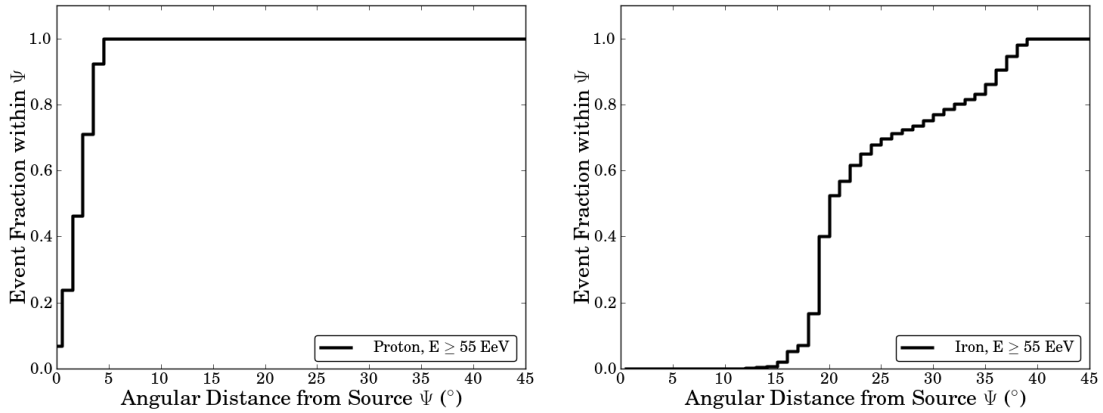

(a) Proton (b) Iron

Figure 3. Cumulative number of simulated events with $E \geq 55$ EeV as a function of angular distance from the direction of the center of Cen A for (a) protons and (b) iron nuclei.

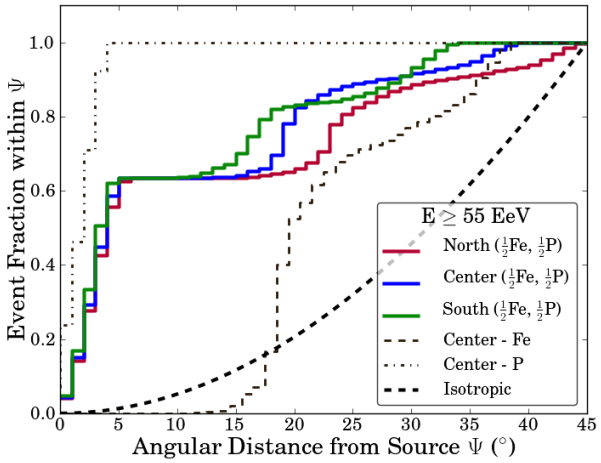

Figure 4. The excess of simulated events near Cen A. The directions have a separation angle up to 45°. Event excess from center, north, and south of Cen A are shown. The thick dashed line shows the expected isotropic flux. The thin dashed line shows only iron events. The dot-dashed line shows only proton events.

We plot the normalized cumulative number of protons and iron nuclei with $E \geq 55$ EeV as a function of angular distance from the direction of Cen A's center in Figure 3. There were no simulated events with arrival directions more than 45° away from the direction of Cen A. The simulated events are weighted by the Auger exposure [23] and an $E^{-2.6}$ differential energy spectrum [24] to match better our simulations to the observations. On average, the magnetic deflections of protons are smaller than those for iron nuclei as expected. Figure 4 shows that there is an excess above the value expected from isotropy both for protons and iron nuclei. This figure also shows that there is a visible excess above the isotropic expectation when combining the two compositions together (50% contributions from each).

We repeat this analysis for events within 3° of the northern and southern tips of Cen A radio lobes. The resulting plot is shown in Figure 4 with different colors. This shows that the excess from Cen A exists regardless of the position of the source along the large radio galaxy, although the excesses are shifted with respect to distance from the source particularly for iron nuclei.

It is evident in all cases that, when considering only the regular component of the GMF, the simulated arrival directions of primary iron nuclei match observations much better than do those from proton primaries. We note that although the angular distance distribution of events looks reasonable (Figures 3 and 4), the Auger excess within about 20° is rather isotropically distributed and does not exhibit the stream-like distribution expected for events originating from Cen A as seen in Figure 2.

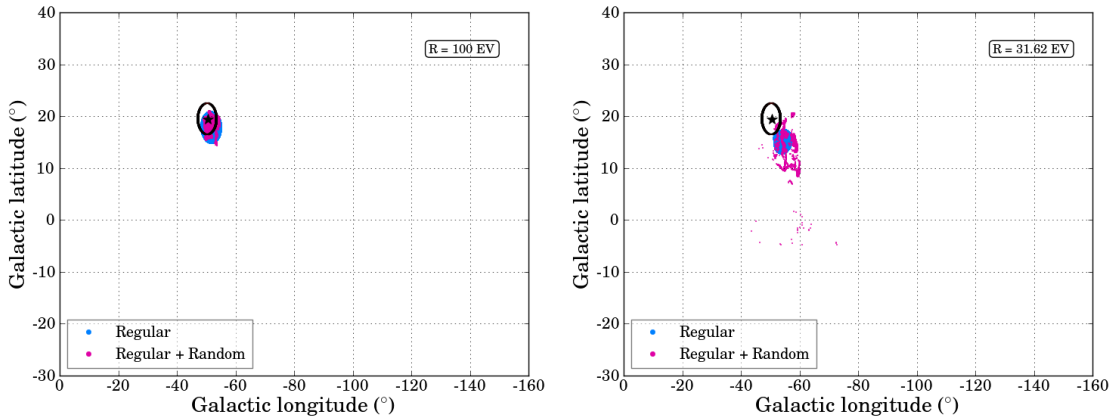

(a) $R = 100$ EV (b) $R = 31.62$ EV

Figure 5. Arrival directions of the simulated events with (a) $R = 100$ EV and (b) $R = 31.62$ EV within 3° of the vicinity of the center of Cen A in regular plus random JF12 GMF model. The blue region relates to events in regular field-only simulation. The black circle shows 3° angular distance from Cen A.

5. UHECR Deflections in JF12 GMF Model including Random Fields

Here we discuss the effects of adding the detailed Kolmogorov random field component (as discussed above in Section 2) to the JF12 regular component. The arrival directions of simulations from the center of Cen A in the JF12 regular component and the JF12 regular-plus-random components are compared in Figures 5 and 6 for $\log(R_{\rm EV}) = 2.0$, 1.5, and 1.0, respectively. Figure 6 also compares two independent realizations of the random field to confirm the consistency of the results. We see that the results of propagation do not change significantly at high rigidities, such as 100 EV and 31.62 EV, between the regular-only and regular-plus-random models. At these rigidities, evaluating events using their average angular position and

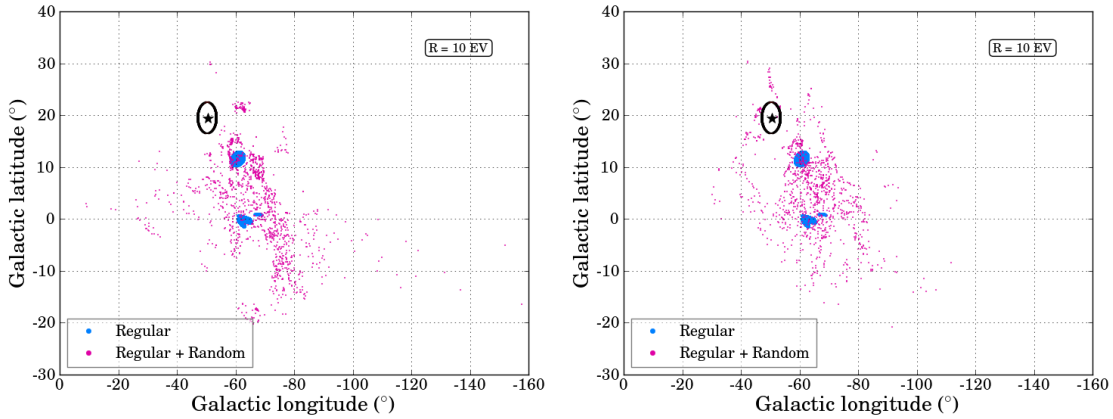

(a) Realization 1 (b) Realization 2

Figure 6. Arrival directions of the simulated events with $R = 10$ EV within 3° of the vicinity of the center of Cen A in the regular field plus (a) the first and (b) the second realization of the Kolmogorov random field. The blue region relates to events in regular field-only simulation. The black circle shows 3° angular distance from Cen A.

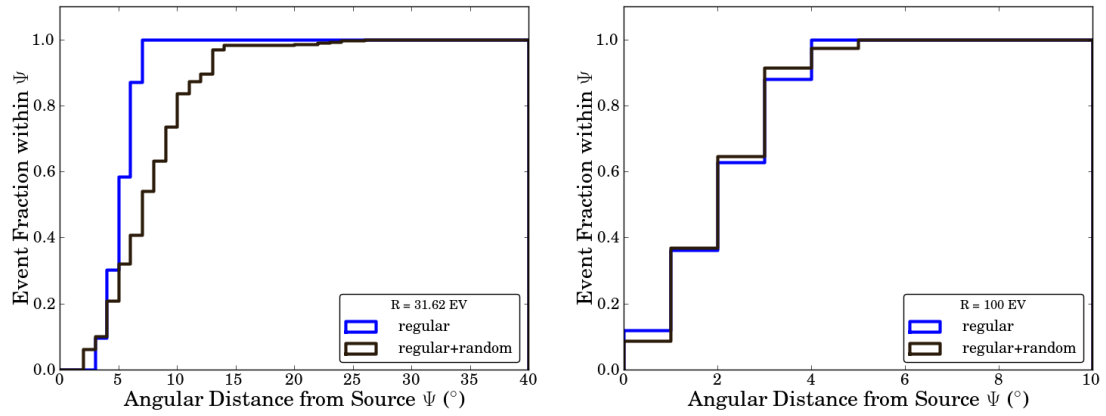

(a) R = 31.62 EV (b) R = 100 EV

Figure 7. Cumulative number of events as a function of angular distance from the direction of the center of Cen A in two cases of regular component and regular-plus-random components of JF12 GMF model. Each figure is for a different rigidity.

standard deviation still works and can be applied for study of the event excesses. At lower rigidities, such as 10 EV, the centroids are separated by a few degrees, but most importantly they are significantly smeared so that studies using just the centroid and standard deviation cannot capture the actual distribution.

The effect of including the Kolmogorov random field as we have done will change the integrated angular distributions shown earlier (Figures 3 and 4). Figure 7 illustrates the effect at two rigidities. At R =31.62 EV, there is a modest but noticeable increase in the width of the integrated angular deviations, whilst at R =100 EV, this effect is negligible. The impact of this will be quite different for the different assumed cases of protons or iron. For protons with energies above 55 EeV, the cumulative histograms (e.g., Figure 4) will show little change.

But iron primaries in the same energy regime have much lower rigidity (as described above, the maximum rigidity used for iron is only $R = 7.08$ EV). It appears that the angular deviation distribution for iron nuclei will widen so much that it will be difficult to resolve it from isotropy. Neither of these cases will resemble observations as well as the outcome of including only the regular JF12 component.

Acknowledgments
Resources supporting this work were provided by the NASA High-End Computing (HEC) Program through the NASA Advanced Supercomputing (NAS) Division at Ames Research Center, consisting of time on the Pleiades supercomputing cluster awarded to Glennys Farrar. We thank Jonathan Roberts and Ronnie Jansson for their collaboration in the initial phase of this work, as well as our many colleagues in the Pierre Auger Collaboration for their many interactions and input. J.M., M.S., and A.K. acknowledge support from the Department of Energy under grants DE-0009926 and DE-FG02-91-EF0617. G.F. acknowledges support from the National Science Foundation and NASA under grants NSF-PHY-1212538 and NNX10AC96G.

References

[1] Zatsepin G T and Kuz'min V A 1966 *Sov. J. Exp. Theor. Phys. Lett.* **4** 78
[2] Greisen K 1966 *Phys. Rev. Lett.* **16** 748
[3] The Pierre Auger Collaboration 2010 *Astropart. Phys.* **34** 314
[4] The Pierre Auger Collaboration 2009 *Astropart. Phys.* **31** 399
[5] Jansson R and Farrar G R 2012 *Astrophys. J.* **757** 14
[6] Jansson R and Farrar G R 2012 *Astrophys. J.* **761** L11
[7] Farrar G R *et al.* 2013 *JCAP* **01** 023F
[8] Farrar G R and Piran T 2000 *ArXiv: astro-ph/0010370*
[9] Ginzburg V L and Syrovatskii S L 1963 *Soviet Astronomy* **7** 357
[10] Gorbunov D S *et al.* 2008 *ArXiv: astro-ph/0804.1088*
[11] Wibig T and Wolfendale A W 2009 Open Astron. J. **2** 95
[12] Hardcastle M J *et al. MNRAS* **393** 1041
[13] Kachelrieß M *et al.* 2009 *New Journal of Physics* **11** 065017
[14] Rachen J P 2008 *XXth Rencontres de Blois, Challenges in Particle Astrophysics*
[15] Fargion D 2008 *Physica Scripta* **78** 045901
[16] Fargion D 2009 *ArXiv: 0908.2650*
[17] Rieger F M and Aharonian F A 2009 *Astron. & Astrophys.* **506** L41
[18] Moskalenko I V *et al.* 2009 *Astrophys. J.* **693** 1261
[19] Nagar N M and Matulich J 2010 *Astron. & Astrophys.* **523** A49
[20] Gold B *et al.* 2011 *Astrophys. J.* **192** 15
[21] Sutherland M *et al.* 2010 *Astropart. Phys.* **34** 198
[22] HEALPix, http://healpix.jpl.nasa.gov/
[23] Sommers P 2001 *Astropart. Phys.* **14** 271
[24] Schulz A for the Pierre Auger Collaboration 2013 *Proc. of the 33rd Int. Cosmic Ray Conf.* arXiv:1307.5059